

# Cosmic tides in view of halos

Tian-Xiang Mao,<sup>1,2</sup> Hong-Ming Zhu,<sup>1,2</sup> Ue-Li Pen,<sup>3,4,5,6</sup> Yu Yu,<sup>7</sup> Xuelei Chen,<sup>1,2,8</sup> and Jie Wang<sup>1</sup>

<sup>1</sup>*Key Laboratory for Computational Astrophysics, National Astronomical Observatories,  
Chinese Academy of Sciences, 20A Datun Road, Beijing 100012, China*

<sup>2</sup>*University of Chinese Academy of Sciences, Beijing 100049, China*

<sup>3</sup>*Canadian Institute for Theoretical Astrophysics, University of Toronto,  
60 St. George Street, Toronto, Ontario M5S 3H8, Canada*

<sup>4</sup>*Dunlap Institute for Astronomy and Astrophysics, University of Toronto,  
50 St. George Street, Toronto, Ontario M5S 3H8, Canada*

<sup>5</sup>*Canadian Institute for Advanced Research, CIFAR Program in  
Gravitation and Cosmology, Toronto, Ontario M5G 1Z8, Canada*

<sup>6</sup>*Perimeter Institute for Theoretical Physics, 31 Caroline Street North, Waterloo, Ontario, N2L 2Y5, Canada*

<sup>7</sup>*Key laboratory for research in galaxies and cosmology, Shanghai Astronomical Observatory,  
Chinese Academy of Sciences, 80 Nandan Road, Shanghai 200030, China*

<sup>8</sup>*Center of High Energy Physics, Peking University, Beijing 100871, China*

(Dated: September 21, 2016)

PACS numbers:

## I. INTRODUCTION

The large-scale structure contains a wealth of information about our Universe, including cosmic acceleration, neutrino masses and inflation. By measuring large-scale structure we can attempt to find the answers to such fundamental questions as what the initial conditions for the Universe are and what the future of the Universe will be. However, the nonlinear evolution and many observational problems make it difficult to extract cosmological information. In our previous studies [1, 2], the gravitational coupling between the long wavelength tidal field and small scale density fluctuations is used to reconstruct the large-scale density field, which provides a new method (cosmic tidal reconstruction) to extract the large-scale information from local observation.

The basic idea of the cosmic tidal reconstruction is that the local anisotropic structure includes the large scale information because of the tidal interactions in different scale modes. Each independent measurement of the small scale power spectrum gives some information about the power spectrum on large scales. So we can use cheaper local observation to estimate the long wavelength tidal field by cosmic tidal reconstruction, which can be used to recover lost 21cm modes and reduce sample variance [1]. We have tested the reconstruction with simulated dark matter density fields [2] and have developed a three-dimensional (3D) method which obtains even better result (in preparation). However, the reconstruction with dark matter density field can not help us to extend this method to actual data in surveys and more effects should be done.

Galaxy survey is one of the leading methods to measure the clustering of dark matter and has been

Dark matter halos, which host observable galaxies and galaxy clusters, are biased tracers of the underlying dark

matter density field. The relation between the galaxy and dark matter halos be described by the halo model [3–5]. Therefore, understanding tidal reconstruction in view of halo field is important for us to extract information from galaxy surveys, which we will study in our next work. In this paper, we extend 3D tidal reconstruction in view of halos and try to reconstruction with a bias-weighting halos field to get a higher correlation between reconstructed and original density field. (\*)

In our previous studies [1, 2], we applied a Gaussianization technique to suppress the large weight of the high density regions because of the quadratic estimator. However, for the halos fields, there is not such a high fluctuation. So we have a good reconstruction even without Gaussianization and which gives us a simpler and clearer physical images. Furthermore, without Gaussianization, we can estimator the bias of tidal reconstruction easily and correct it, which is import for our reconstruction.

The shot noise, which due to the discrete sampling of halos, is another problem that should be solved. Generally speaking, we assume the shot noise is the inverse of the number density  $\bar{n}$ . So for the dark matter density field, the shot noise is too small to ignore. However, the influence of the shot noise limits the result of reconstruction in view of hales. Here, we apply a wiener filter to suppress the shot noise, which we will introduce later.

Galaxy survey has been one of the leading methods to measure the clustering of dark matter. There have been a lot of efforts in developing optimal weighting in galaxy survey [6–10]. It is difficult to get the mass information in galaxy survey. However we can apply a biased weighting, that bias can be given by galaxy luminosity, to improve the signal to noise ratio of the

halo fields. In this paper, we are not try to find a optimal bias weighting, but the optimal weighting may be needed in some case.

(\*)This paper is organized as follows. In Section II, we review the reconstruction technique. In Section III, we study the performance of reconstruction in halo density fields from  $N$ -body simulations. In Section IV, we study how much improvement can get from bias weighted halo fields.

## II. REVIEW OF TIDAL RECONSTRUCTION

The basic idea of cosmic tidal reconstruction is presented originally in Ref. [1] and detailed description can be found in Ref. [2]. In this section we will briefly review it.

Not only the small-scale density fluctuation but also the long-wavelength tidal field influence the evolution of local small-scale density field. So we can use small scale observations to solve the large scale tidal shear and gravitational potential. If we just assume the leading-order coupling between the long-wavelength tidal field and small-scale density field, the tidal distortion of the local small-scale power spectra can be written as

$$P(\mathbf{k}, \tau)|_{t_{ij}} = P_{1s}(k, \tau) + \hat{k}^i \hat{k}^j t_{ij}^{(0)} P_{1s}(k, \tau) f(k, \tau), \quad (1)$$

where  $\hat{k}$  is the unit vector in the direction of  $\mathbf{k}$ ,  $P_{1s}$  is the small-scale power spectrum, the long-wavelength tidal field is  $t_{ij} = \Phi_{L,ij} - \delta_{ij} \nabla^2 \Phi_L / 3$  and  $f(k, \tau)$  are used to describe the coupling of the long-wavelength tidal field and small-scale density field. In this paper, we use superscript (0) and  $\tau$  to denotes the "initial" time and conformal time, respectively.

The filter  $f(\mathbf{k}, \tau)$  is defined as

$$f(\mathbf{k}, \tau) = 2\alpha - \beta \frac{d \ln P_{1s}(k, \tau)}{d \ln k}, \quad (2)$$

where

$$\begin{aligned} \alpha(\tau) &= -D_{\sigma 1}(\tau) + F(\tau), \\ \beta(\tau) &= F(\tau), \end{aligned} \quad (3)$$

with

$$D_{\sigma 1}(\tau) = \int_0^\tau d\tau' \frac{H(\tau)D(\tau') - H\tau'D\tau}{\dot{H}(\tau')D(\tau') - H(\tau')\dot{D}(\tau')} \frac{T(\tau')D(\tau')}{D(\tau)}, \quad (4)$$

$$F(\tau) = \int_0^\tau d\tau'' a(\tau'') T(\tau'') \int_{\tau''}^\tau d\tau' / a(\tau'). \quad (5)$$

Here,  $D(\tau)$  is the linear growth function,  $T(\tau) = D(\tau)/a(\tau)$  is the linear transfer function

and  $H(\tau) = d \ln a / d\tau$  is the comoving Hubble parameter.

From Eq. (1), we express small-scale density fluctuations with the long-wavelength tidal field  $t_{ij}$  and local small-scale density field  $\delta_{1s}$ . Then a tidal shear estimator can be constructed as following.

The tidal tensor  $t_{ij}$  can be decomposed as

$$t_{ij} = \begin{pmatrix} \gamma_1 - \gamma_z & \gamma_2 & \gamma_x \\ \gamma_2 & -\gamma_1 - \gamma_z & \gamma_y \\ \gamma_x & \gamma_y & 2\gamma_z \end{pmatrix}, \quad (6)$$

where  $\gamma_1 = (\Phi_{L,11} - \Phi_{L,22})/2$ ,  $\gamma_2 = \Phi_{L,12}$ ,  $\gamma_x = \Phi_{L,13}$ ,  $\gamma_y = \Phi_{L,23}$ ,  $\gamma_z = (2\Phi_{L,23} - \Phi_{L,11} - \Phi_{L,22})/6$ .

In 3D reconstruction,

$$\begin{aligned} \hat{\gamma}_1 &= [\delta_g^{w_1}(x) \delta_g^{w_1}(x) - \delta_g^{w_2}(x) \delta_g^{w_2}(x)], \\ \hat{\gamma}_2 &= [2\delta_g^{w_1}(x) \delta_g^{w_2}(x)], \\ \hat{\gamma}_x &= [2\delta_g^{w_1}(x) \delta_g^{w_3}(x)], \\ \hat{\gamma}_y &= [2\delta_g^{w_2}(x) \delta_g^{w_3}(x)], \\ \hat{\gamma}_z &= [2\delta_g^{w_3}(x) \delta_g^{w_3}(x) - \delta_g^{w_1}(x) \delta_g^{w_1}(x) - \delta_g^{w_2}(x) \delta_g^{w_2}(x)]/3, \end{aligned} \quad (7)$$

where  $\delta_g^{w_i}(x)$  is a filtered density fields, and  $i$  indicates  $\hat{x}, \hat{y}, \hat{z}$  directions. In Fourier space  $w_i$  is given by

$$\delta_g^{w_i}(\mathbf{k}) = \delta_g(\mathbf{k}) w_i(\mathbf{k}). \quad (8)$$

Here  $\delta_g$  is the Gaussianized density field and  $w_i(\mathbf{k})$  is a optimal filter, defined as

$$w_i(\mathbf{k}) = i \hat{k}_i \left[ \frac{P(k) f(k)}{Q P_{tot}^2(k)} \right]^{1/2}, \quad (9)$$

with

$$Q = \int \frac{2k^2 dk}{15\pi^2} \frac{P^2(k)}{P_{tot}^2(k)} f^2(k) \quad (10)$$

and

$$P_{tot}(k) = P(k) + P_N(k) \quad (11)$$

is the observed power spectrum which includes both signal and noise. The filter  $f(k)$  is from Eq. (2).

Then the reconstructed 3D convergence field is

$$\begin{aligned} \kappa_{3D}(\mathbf{k}) &= \frac{1}{k^2} [(k_1^2 - k_2^2) \gamma_1(\mathbf{k}) + 2k_1 k_2 \gamma_2(\mathbf{k}) + 2k_1 k_3 \gamma_x(\mathbf{k}) \\ &\quad + 2k_2 k_3 \gamma_y(\mathbf{k}) + (2k_3^2 - k_1^2 - k_2^2) \gamma_z(\mathbf{k})]. \end{aligned} \quad (12)$$

To correct the bias and reduce the noise in reconstructed field, we write the reconstructed clean field  $\hat{\kappa}$  as

$$\hat{\kappa}(k_\perp, k_\parallel) = \frac{\kappa_{3D}(k_\perp, k_\parallel)}{b(k_\perp, k_\parallel)} W(k_\perp, k_\parallel), \quad (13)$$

where bias factor

$$b(k_{\perp}, k_{\parallel}) = \frac{P_{\kappa 3D\delta}(k_{\perp}, k_{\parallel})}{P_{\delta}(k_{\perp}, k_{\parallel})} \quad (14)$$

and Wiener filter

$$W(k_{\perp}, k_{\parallel}) = \frac{P_{\delta}(k_{\perp}, k_{\parallel})}{P_{\kappa 3D}(k_{\perp}, k_{\parallel})/b^2(k_{\perp}, k_{\parallel})}. \quad (15)$$

Here, the noise power spectrum is

$$P_n(k_{\perp}, k_{\parallel}) = P_{\kappa 3D}(k_{\perp}, k_{\parallel}) - b^2(k_{\perp}, k_{\parallel})P_{\delta}(k_{\perp}, k_{\parallel}). \quad (16)$$

### III. PERFORMANCE OF RECONSTRUCTION

We have discussed the tidal reconstruction with local dark matter density field with 2D and 3D method [2]. In practice, however, we can only observe galaxies instead of dark matter density fields. And the distribution of halo is a biased tracer of the underlying dark matter density. Therefore, the reconstruction in view of halo is even more relevant to the observation.

In this section we perform reconstruction in simulated halos fields, following the same process in the previous paper. And we also use the cross correlation coefficient to quantify the result of reconstruction.

#### A. Simulation

We run N-body simulations using the CUBEP<sup>3</sup>M code with  $2048^3$  dark matter particles in a box of side length  $L = 1.2$  Gpc/h. We have adopted the following set of cosmological parameter values:  $\Omega_b = 0.049$ ,  $\Omega_c = 0.259$ ,  $h = 0.678$ ,  $A_s = 2.139 \times 10^{-9}$  and  $n_s = 0.968$ . Ten runs with independent initial conditions were performed to provide better statistics. In the following calculations we use outputs at  $z = 0$ .

As we have shown before, the purpose of tidal reconstruction is trying to reconstruct the large-scale tidal field from local small-scale density field. In the following of this subsection, we show the shot noise and the inverse signal to noise ratio (N/S) to help us understand that how much information we can obtain from different halo fields.

#### B. Reconstruction

The performance of reconstruction we mainly follow our previous works [1, 2]. However, there are some changes because of the difference between the dark matter and halo fields. The algorithm of the reconstruction

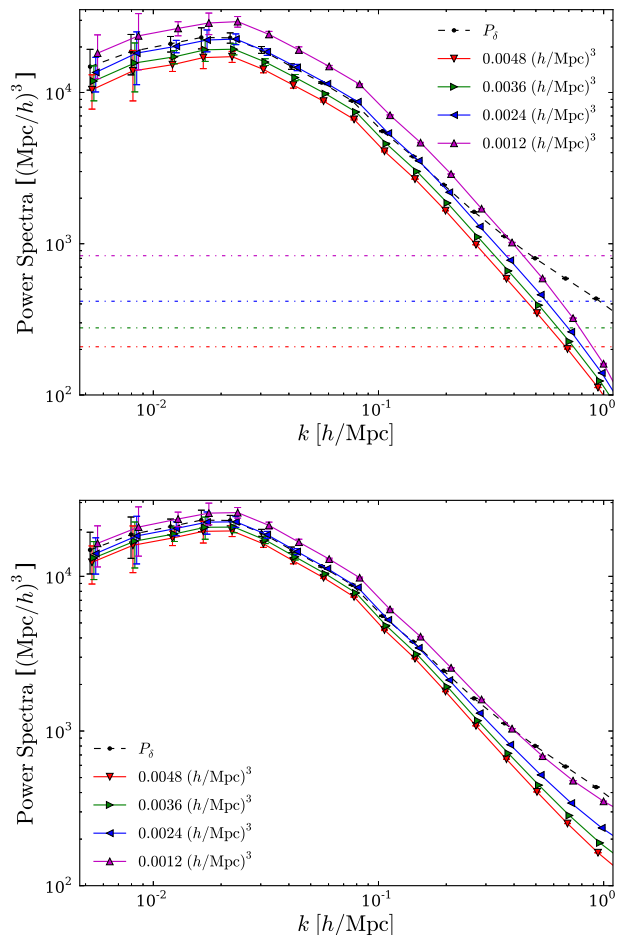


FIG. 1: Top panel: the auto-power spectrum of halo fields. The solid lines are the power spectrum of halo fields with number density of  $0.0048 \text{ h}^3 \text{Mpc}^{-3}$ ,  $0.0036 \text{ h}^3 \text{Mpc}^{-3}$ ,  $0.0024 \text{ h}^3 \text{Mpc}^{-3}$  and  $0.0012 \text{ h}^3 \text{Mpc}^{-3}$ , respectively. The horizontal dot dash lines are corresponding shot noise  $1/\bar{n}$  for every halo fields. Here  $\bar{n}$  is the number density. The black dashed line is the power spectrum of dark matter field. Bottom panel: same as the top panel, but the colored solid lines are the matter-halo cross power spectrum.

in view of halo is as follows.

- (i). Convolution the halo density field with a wiener filter  $W$  defined as

$$W(k) = \frac{P_{\delta}(k)}{(P_h(k) + 1/\bar{n})/b^2}, \quad (17)$$

where  $P_h$ ,  $P_{\delta}$  and  $\bar{n}$  are the auto-power spectrum of halo and dark matter fields and the number density of the halo field. The bias factor  $b$  is a  $k$ -independent bias and here we calculate it by averaging the bias in the first six  $k$ -bins where  $k < 0.04 \text{ h/Mpc}$ .

Here, the top we use  $b^2 P_{\delta}$  instead of  $P_h$  because we consider the signal is the dark matter density field not the halo field, although we use the halo field trace the dark

matter density field. After applied Eq. (17), we suppress the noise in halo field (both the shot noise and ). Then we obtain the filtered halo density field  $\tilde{\delta}_h$ .

(ii). Applying a Gaussian smoothing kernel to smooth filtered halo density field:

$$\bar{\delta}(\mathbf{x}) = \int d^3x' \mathbf{S}(\mathbf{x} - \mathbf{x}') \delta(\mathbf{x}'), \quad (18)$$

where  $\mathbf{S}(r) = e^{-r^2/2R^2}$ . Here, we calculated a lots of different smoothing scale and find we can obtain the optimal reconstruction result with the smoothing scale of  $R = 1.0 \text{ Mpc}/h$ . So we select  $R = 1.0 \text{ Mpc}/h$  as the smoothing scale in this paper. By this step, we get a smoothed field  $\tilde{\delta}_h$  as matter density field which will be used in later reconstruction and which is suppressed the vary small-scale fluctuations.

(iii). Then, we convolve the filtered and smoothed density field  $\tilde{\delta}_h$  and calculate  $\gamma_1, \gamma_2, \gamma_x, \gamma_y, \gamma_z$ , by Eq. (7)(9)(10). And from Eq. (12) we obtain 3D convergence field  $\kappa_{3D}(\mathbf{k})$ .

(iv). To calculate  $b(k_\perp, k_\parallel)$  and  $W(k_\perp, k_\parallel)$  to correct the estimated  $\kappa_{3D}$ , we estimate the power spectrum  $P_{\kappa_{3D}}$  and  $P_{\kappa_{3D}\delta}$  use these ten simulations. Then we obtain the reconstructed  $\kappa(\mathbf{k})$  from Eq. (13).

In this paper, we remove the step of Gaussianization in our reconstruction. This is because there are not such huge fluctuations in halos fields compare to dark matter density fields. We applied Gaussianization smoothing kernel in reconstruction with dark matter density field to avoid the effect because of the huge small-scale fluctuations. However, in halo fields reconstruction, we obtain a batter result without Gaussianization.

### C. Result

In this subsection, we show the correlation coefficient, bias and noise of reconstruction.

The correlation coefficient we defined as

$$r(k) = \frac{P_{\delta\kappa}(k)}{\sqrt{P_{\delta\delta}(k)P_{\kappa\kappa}(k)}}, \quad (19)$$

and the bias factor is

$$b(k) = \frac{P_{\delta\kappa}(k)}{P_{\delta\delta}(k)} \quad (20)$$

In Fig. 4, we show the bias of reconstruction. To quantify the bias of our reconstruction by Eq. (20), we need to calculate the  $Q$  factor in Eq. (10) and correct the bias of halos and matter fields  $b_h = P_{\delta h}/P_{\delta\delta}$ .

Because of the smoothing kernel we used in Eq. (18), the  $Q$  factor becomes:

$$Q = \int \frac{2k^2 dk}{15\pi^2} W^2(k) S^2(k) f^2(k), \quad (21)$$

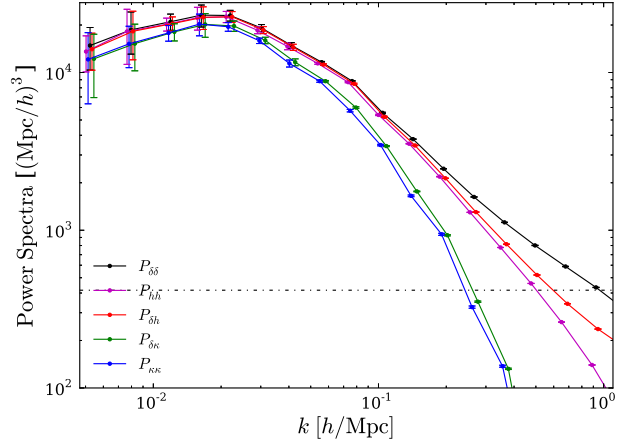


FIG. 2: Auto-power spectrum of dark matter, halo and reconstructed  $\kappa$  fields and cross-power spectrum of matter-halo and matter-kappa, respectively. Here the number density of halo fields is  $0.0024 \text{ h}^3 \text{ Mpc}^{-3}$  and the smoothing scale is  $R = 1.0 \text{ Mpc}/h$ .

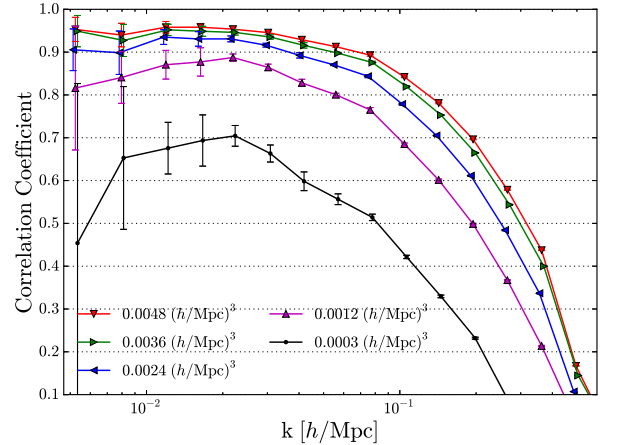


FIG. 3: Correlation coefficient of reconstructed tidal field  $\kappa$  and dark matter density field  $\delta$  (Eq. (19)). Here we choose the number density of halos fields as  $0.0012 \text{ h}^3 \text{ Mpc}^{-3}$ ,  $0.0024 \text{ h}^3 \text{ Mpc}^{-3}$ ,  $0.0036 \text{ h}^3 \text{ Mpc}^{-3}$  and  $0.0048 \text{ h}^3 \text{ Mpc}^{-3}$  and apply a smoothing kernel with  $R = 1.0 \text{ Mpc}/h$  (Eq. (18)). We also plot the correlation coefficient of the reconstructed field from halo fields with number density of  $0.0003 \text{ h}^3 \text{ Mpc}^{-3}$ , which is the average number density of BOSS.

where  $S(k)$  is the smoothing kernel in  $k$  space and  $W(k)$  is the wiener filter in Eq. (17). Here, we solve the  $Q$  factor by a interval from the smallest  $k$  to the Nyquist frequency in our cube of simulation.

Then we can obtain the bias of reconstruction

$$b_{\text{rec}} = \frac{P_{\kappa_{3D}\delta}}{P_{\delta\delta}} \frac{1}{b_0^2 Q}, \quad (22)$$

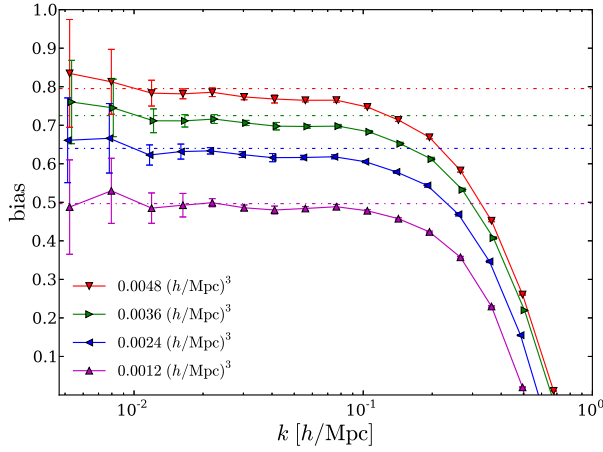


FIG. 4: Bias factor  $b(k)$  of reconstructed  $\kappa$  field from different number density halo fields (Eq. (20)). Here we correct the bias by Eq. (22) and get the constant bias of reconstruction as 0.795, 0.725, 0.640 and 0.497 for reconstructed  $\kappa$  fields from  $0.0048 h^3 \text{Mpc}^{-3}$ ,  $0.0036 h^3 \text{Mpc}^{-3}$ ,  $0.0024 h^3 \text{Mpc}^{-3}$  and  $0.0012 h^3 \text{Mpc}^{-3}$ , respectively. Here, the constant bias is obtained by averaging the bias of the first 6  $k$ -bins.

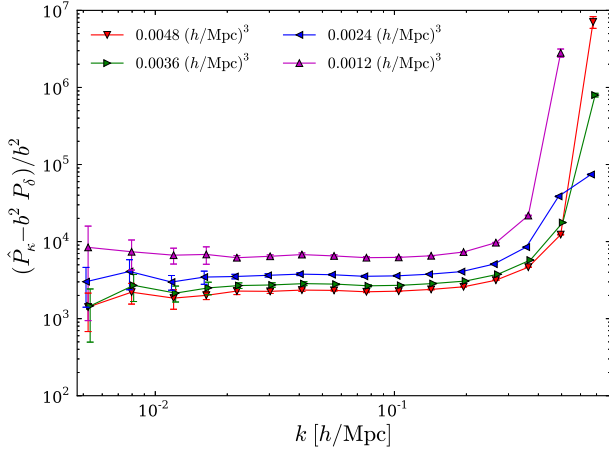


FIG. 5: The noise spectrum of reconstruction. Here we define the noise spectrum as  $P_n(k) = P_\kappa(k)/b^2(k) - P_\delta(k)$  and the bias  $b(k) = P_{\kappa\delta}(k)/P_{\delta\delta}(k)$  is a  $k$ -dependent bias. Four colored solid lines are corresponding different number density of halos fields.

here,  $b_0$  is the  $k$ -independent bias of simulated halo fields.

#### IV. THE CROSS TERM OF $\gamma$

We can estimate the  $\gamma$  shear from Eq. (7). If we separate halo field  $\delta$  into two mass bins, such as

$$\delta = \delta_a + \delta_b, \quad (23)$$

where subscript  $a$  and  $b$  indicate two mass bins with the same number density. Obviously, we can obtain  $\gamma_i^a$  and

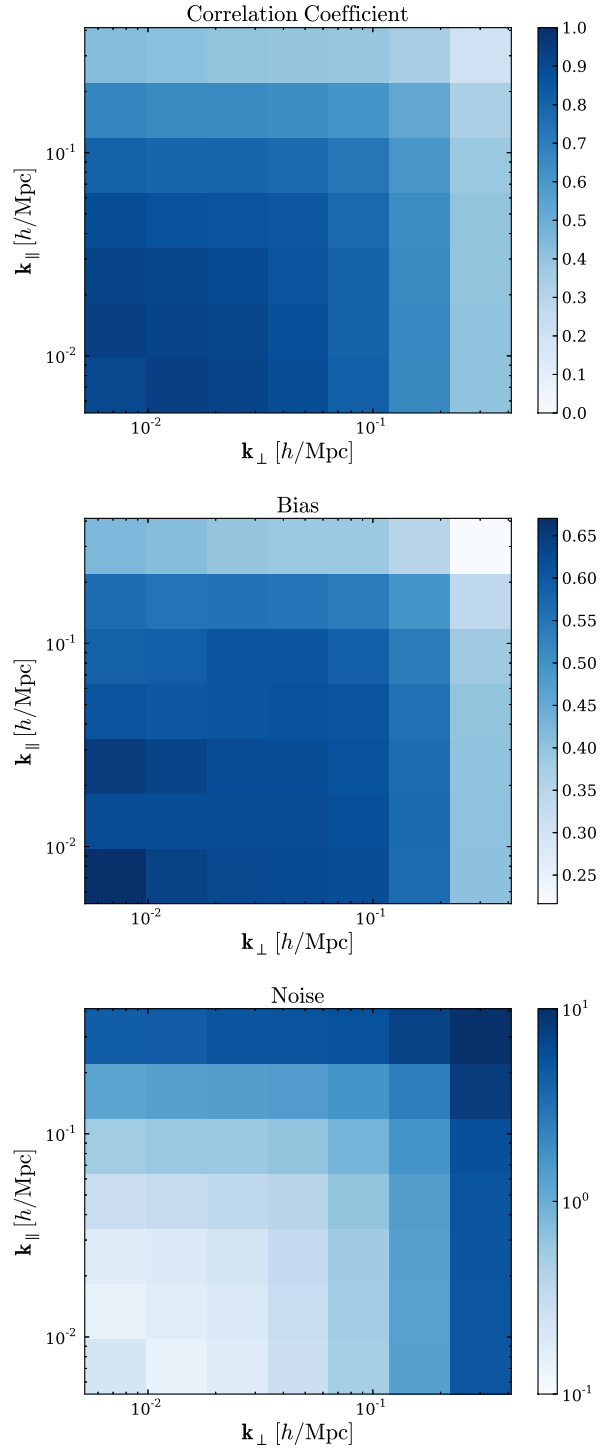


FIG. 6: We plot the 2D correlation coefficient, bias factor and noise of reconstructed  $\kappa$  field from top to bottom, respectively. Here the definition of correlation coefficient and bias factor are same with Fig. 3 and Fig. 4, and the noise in the bottom panel is defined as  $(P_\kappa - b^2 P_\delta)/b^2 P_\delta$ . All three panels are reconstructed from halo fields with number density of  $0.0024 h^3 \text{Mpc}^{-3}$ .

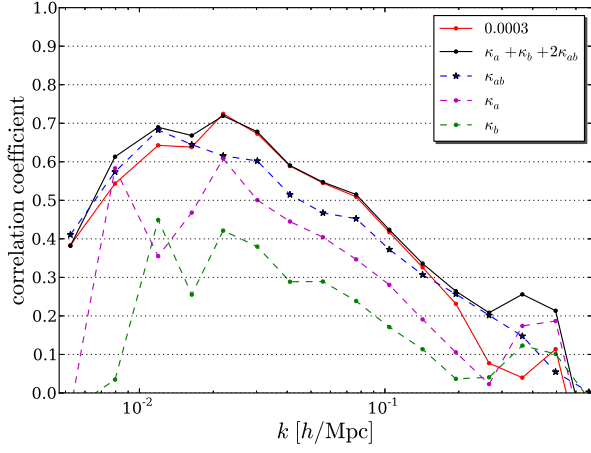


FIG. 7: Reconstruction by Eq. (25). We separate the  $\bar{n} = 0.0003 \, h^3 \text{Mpc}^{-3}$  halos field into two mass bins  $\delta_a$  and  $\delta_b$  and reconstruct the  $\kappa$  field.

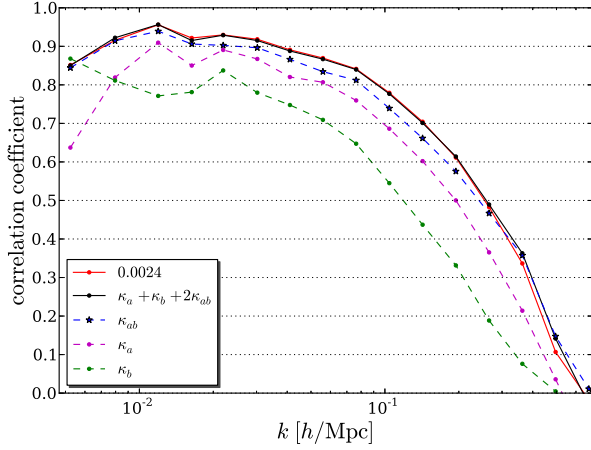


FIG. 8: Identical to Fig. 7, but the number density of separated halo field is  $0.0024 \, h^3 \text{Mpc}^{-3}$ .

$\gamma_i^b$  by Eq. (7). Here index  $i$  indicates '1', '2', 'x', 'y', 'z'. In addition, we can also estimate the  $\gamma$  field cross  $\delta_a$  and  $\delta_b$ .

The cross term of  $\gamma$  can be

$$\begin{aligned}\hat{\gamma}_1 &= [\delta_a^{w_1}(x)\delta_b^{w_1}(x) - \delta_a^{w_2}(x)\delta_b^{w_2}(x)], \\ \hat{\gamma}_2 &= [\delta_a^{w_1}(x)\delta_b^{w_2}(x) + \delta_b^{w_1}(x)\delta_a^{w_2}(x)], \\ \hat{\gamma}_x &= [\delta_a^{w_1}(x)\delta_b^{w_3}(x) + \delta_b^{w_1}(x)\delta_a^{w_3}(x)], \\ \hat{\gamma}_y &= [\delta_a^{w_2}(x)\delta_b^{w_3}(x) + \delta_b^{w_2}(x)\delta_a^{w_3}(x)], \\ \hat{\gamma}_z &= [(2\delta_a^{w_3}(x)\delta_b^{w_3}(x) - \delta_a^{w_1}(x)\delta_b^{w_1}(x) - \delta_a^{w_2}(x)\delta_b^{w_2}(x)]/3,\end{aligned}\quad (24)$$

and the final reconstructed  $\kappa$  field is

$$\kappa = \kappa_a + \kappa_b + 2\kappa_{ab} \quad (25)$$

[1] U.-L. Pen, R. Sheth, J. Harnois-Deraps, X. Chen, and Z. Li, ArXiv e-prints (2012), 1202.5804.  
[2] H.-M. Zhu, U.-L. Pen, Y. Yu, X. Er, and X. Chen, ArXiv e-prints (2015), 1511.04680.  
[3] R. Scoccimarro, R. K. Sheth, L. Hui, and B. Jain, *Astrophys. J.* **546**, 20 (2001), astro-ph/0006319.  
[4] J. A. Peacock and R. E. Smith, *Mon. Not. R. Astron. Soc.* **318**, 1144 (2000), astro-ph/0005010.  
[5] U. Seljak, *Mon. Not. R. Astron. Soc.* **318**, 203 (2000), astro-ph/0001493.  
[6] W. J. Percival, L. Verde, and J. A. Peacock, *Mon. Not.*

*R. Astron. Soc.* **347**, 645 (2004), astro-ph/0306511.  
[7] U. Seljak, N. Hamaus, and V. Desjacques, *Physical Review Letters* **103**, 091303 (2009), 0904.2963.  
[8] N. Hamaus, U. Seljak, V. Desjacques, R. E. Smith, and T. Baldauf, *Phys. Rev. D* **82**, 043515 (2010), 1004.5377.  
[9] N. Hamaus, U. Seljak, and V. Desjacques, *Phys. Rev. D* **86**, 103513 (2012), 1207.1102.  
[10] R. E. Smith and L. Marian, *Mon. Not. R. Astron. Soc.* **454**, 1266 (2015), 1503.06830.